Applied Catalysis B: Environmental 180 (2016) 227–236

Contents lists available at ScienceDirect

Applied Catalysis B: Environmental

journal homepage: www.elsevier.com/locate/apcatb

Routes for the electrochemical degradation of the artificial food azo-colour Ponceau 4R by advanced oxidation processes

Abdoulaye Thiam, Enric Brillas, José A. Garrido, Rosa M. Rodríguez, Ignasi Sirés*

Laboratori d'Electroquímica dels Materials i del Medi Ambient, Departament de Química Física, Facultat de Química, Universitat de Barcelona, Martí i Franquès 1-11, 08028 Barcelona, Spain

ARTICLE INFO

Article history:
Received 2 May 2015
Received in revised form 13 June 2015
Accepted 19 June 2015
Available online 23 June 2015

Keywords:
Acid Red 18
BDD anode
Catalyzed EAOPs
Food colours
Reaction pathways

ABSTRACT

The performance of three electrochemical advanced oxidation processes, namely electro-oxidation with electrogenerated H_2O_2 (EO–H_2O_2), electro-Fenton (EF) and photoelectro-Fenton (PEF) for the treatment of aqueous solutions of the food azo dye Ponceau 4R in an undivided cell with a BDD anode and an air-diffusion cathode was compared in terms of colour, dye concentration and total organic carbon (TOC) removals. PEF treatments in ultrapure water with Na_2SO_4 were performed to assess the effect of current density, as well as supporting electrolyte and dye concentrations. At 100 mA cm^{-2}, solutions of 130 mL of 254 mg L^{-1} of the dye in 0.05 M Na_2SO_4 became colourless and totally mineralized after 50 and 240 min, respectively, which can be explained by the synergistic action of BDD(•OH) at the anode surface and homogeneous •OH formed in the bulk from Fenton's reaction promoted in the presence of Fe^{2+} catalyst. Furthermore, UVA photons induced the continuous Fe^{2+} regeneration and photolytic decomposition of refractory intermediate complexes. In that aqueous matrix, the cleavage of the dye molecules proceeded through several reaction routes to yield *N*-containing and non-*N*-containing derivatives with one or two aromatic rings, short-chain aliphatic carboxylic acids and inorganic ions. Oxalic and oxamic acids and sulfate ions were accumulated at different rates in EO–H_2O_2, EF and PEF. The three methods allowed the progressive decontamination of Ponceau 4R solutions in a real water matrix even without the addition of electrolyte, although complete TOC abatement after 360 min at 33.3 mA cm^{-2} was only ensured by the iron-catalyzed PEF process.

1. Introduction

Currently, food additives such as preservatives and colouring agents are among top food safety concerns in industrialized countries, despite being carefully regulated by national and international authorities. Indeed, their effects become uncontrolled when unintended targets, particularly children or some highly sensitive person (HSP) with allergies or food intolerances, are routinely exposed to them upon drinking water consumption. According to the International Food Information Council (IFIC) and the US Food and Drug Administration (FDA), colour additives include dyes, pigments and any other substance applied to a food, drug, cosmetic or the human body to impart colour [1]. Azo compounds are the most widespread synthetic colouring substances in the food industry, as occurs in many other sectors [2,3], but the negative impact of the so-called food azo-colours has been much less investigated than that of their textile counterparts so far. These dyes present one or more azo (—N=N—) bonds and usually exhibit complex structures that confer them large stability against physicochemical attack and bio/photodegradation, thus becoming persistent in water [3].

Ponceau 4R ($C_{20}H_{11}N_2O_{10}S_3Na_3$, trisodium 2-hydroxy-1-(4-sulphonato-1-naphthylazo)-naphthalene-6,8-disulphonate, also known as Acid Red 18, New Coccine or additive E124 in the industry, CI 16255, λ_{max} = 508 nm) is a paradigmatic case of sulphonated azo dye employed to give red colouring to foodstuffs. Lately, serious concerns have arisen since the intake of Ponceau 4R is plausibly connected to asthma and insomnia and it may increase children's hyperactivity and intolerance [4]. As a result, in 2009, the European Food Safety Authority reduced the acceptable daily intake from 4.0 to 0.7 mg (kg body weight)$^{-1}$ [5]. Despite being negative in in vitro genotoxicity as well as in long-term carcinogenicity studies, the topic is still controversial [6]. For instance, Ponceau 4R is currently not approved in the United States, Canada, Norway and Finland, and it is listed as a banned substance by some authorities [7]. Since information about the safety of water containing Ponceau 4R and other related azo dyes

* Corresponding author. Fax: +34 934021231.
E-mail address: i.sires@ub.edu (I. Sirés).

http://dx.doi.org/10.1016/j.apcatb.2015.06.039
0926-3373/

remains inconclusive [8], the best way to reduce risks is to develop much more effective water treatment technologies that ensure their complete removal before reaching end users. The great ability of advanced oxidation processes (AOPs) such as heterogeneous photocatalysis [9,10], ozone-electrolysis with Pt anode [11], chemical Fenton's reagent [12,13] and photo-Fenton [13] to degrade Ponceau 4R has been demonstrated. For the two latter Fenton-based AOPs, however, scarce information was provided, only describing a similar decolourization and mineralization rate in ultrapure water in both cases. Note that those studies did not evaluate the possible influence of a more complex water matrix and the formation of by-products, which is crucial for establishing the actual viability of both techniques. Conversely, to the best of the authors' knowledge, the performance of the electrochemical AOPs (EAOPs) to destroy this dye has not been reported yet.

In the last decade, considerable effort has been devoted to the study of fundamentals and scale-up of electrochemical technologies for wastewater treatment, especially focusing on the destruction of organic matter by hydroxyl radicals [14–16]. Electrooxidation (EO) is the most popular EAOP due to its simplicity, adaptability and outstanding performance of particular setups. This process relies on the electrocatalytic properties of the anode surface (M), since some materials like Pt only favour the partial conversion of contaminants by direct oxidation or under the action of chemisorbed oxides (MO), whereas others like boron-doped diamond (BDD) may promote the complete destruction of organic matter by physisorbed BDD(•OH) formed as follows [17–23]:

$$BDD + H_2O \rightarrow BDD(^{\bullet}OH) + H^+ + e^- \quad (1)$$

The use of undivided cells with a BDD anode and an active cathode can enhance the degree and/or rate of decontamination. Thus, in EO-H_2O_2, an air- or pure O_2-fed airtight or porous carbonaceous cathode is employed to electrogenerate H_2O_2 as follows [24–28]:

$$O_{2(g)} + 2H^+ + 2e^- \rightarrow H_2O_2 \quad (2)$$

H_2O_2 is a weak oxidant, although it can be oxidized to $HO_2^{\bullet}$ at the anode or be further activated in metal-catalyzed EAOPs like electro-Fenton (EF) and photoelectro-Fenton (PEF) [16]. In EF, the presence of low amounts of Fe^{2+} leads to the production of •OH in the bulk through homogeneous catalysis via Fenton's Reaction (3) at optimum pH ~ 3 [29]. Organics are then destroyed upon the synergistic action of heterogeneous and homogeneous catalysis (BDD(•OH) and •OH, respectively).

$$H_2O_2 + Fe^{2+} \rightarrow Fe^{3+} + {}^{\bullet}OH + OH^- \quad (3)$$

If an UVA lamp is used to irradiate the solution in the EF setup, then so-called PEF process, the mineralization is enhanced because UV photons induce the photoreduction of $Fe(OH)^{2+}$ to Fe^{2+} via Reaction (4) and the photolysis of refractory Fe(III)-carboxylate products by Reaction (5) [16,29].

$$Fe(OH)^{2+} + h\nu \rightarrow Fe^{2+} + {}^{\bullet}OH \quad (4)$$

$$Fe(OOCR)^{2+} + h\nu \rightarrow Fe^{2+} + CO_2 + R^{\bullet} \quad (5)$$

BDD anode has an extraordinary oxidation power that favours the production of oxidants such as H_2O_2, O_3, ferrate and peroxosalts ($S_2O_8^{2-}$, $P_2O_8^{4-}$ and $C_2O_6^{2-}$) depending on the aqueous matrix composition [16]. When the treated acidic solution contains Cl^- ions, •OH and/or BDD(•OH) (and UV in PEF) act in concomitance with active chlorine species (Cl_2 and HClO) produced in the bulk via Reactions (6) and (7) [3,14,16]. This medium, which is typical when treating real water matrices, is quite complex since oxychlorine anions [30–32], (oxy) chlorine radicals [33], chloramines [34], trihalomethanes and haloacetic acids [35], as well as refractory chlorinated by-products, can appear.

$$2Cl^- \rightarrow Cl_{2(aq)} + 2e^- \quad (6)$$

$$Cl_{2(aq)} + H_2O \rightarrow HClO + Cl^- + H^+ \quad (7)$$

Encouraging results have been obtained for the treatment of textile azo dyes by EAOPs with a BDD anode [36–40], and very recently we have even discussed the behaviour of two food azo dyes in such systems [41,42]. In the present work, aiming to gain more thorough knowledge about the fate of food azo-colours upon application of EAOPs, Ponceau 4R has been chosen as a model pollutant. It has been comparatively degraded in EO–H_2O_2, EF and PEF systems using an undivided BDD/air-diffusion cell. Most electrolyses have been carried out in ultrapure water with added Na_2SO_4 in order to investigate the effect of parameters like current density (j) and electrolyte and pollutant contents on the colour, dye concentration, and total organic carbon (TOC) removals. The reaction by-products identified by chromatographic techniques have allowed the proposal of various reaction pathways. The viability of the tested EAOPs to degrade Ponceau 4R in a real water matrix in the absence and presence of supporting electrolyte has been ascertained as well.

2. Experimental

2.1. Chemicals

Ponceau 4R (100% content) was purchased from Acros Organics. Anhydrous sodium sulfate, sodium chloride and lithium perchlorate used as supporting electrolytes, as well as iron(II) sulfate heptahydrate used as catalyst in EF and PEF, were of analytical grade supplied by Merck and Fluka. Oxalic, oxamic, fumaric, tartronic, formic and maleic acids used as standards were of analytical grade purchased from Merk, Avocado and Panreac. Sulfuric, hydrochloric and perchloric acids and sodium hydroxide used to regulate the pH were of analytic grade purchased from Merck, Acros Organics and Panreac. Organic solvents and other chemicals used were of high-performance liquid chromatography (HPLC) or analytical grade supplied by Sigma-Aldrich, Lancaster, Merck and Panreac. Solutions were prepared with ultrapure water obtained from a Millipore Milli-Q system with resistivity >18 MΩ cm at 25 °C. Some comparative trials were also carried out with a real water matrix collected from a secondary clarifier of a municipal wastewater treatment plant located in Manresa (Barcelona, Spain). Its main characteristics determined in the laboratory were: pH 7.3, specific conductivity = 1.9 mS cm^{-1} (equivalent to ca. 0.010 M Na_2SO_4), TOC = 25 mg L^{-1}, 1.99 mM SO_4^{2-} and 10.3 mM Cl^-. No iron ions were detected. This water was preserved at 4 °C and used the day after collection.

2.2. Electrochemical cells

The experiments were conducted in an open, undivided, cylindrical glass tank reactor of 150 mL capacity equipped with a double jacket for recirculation of thermostated water at 25 °C. The anode was a BDD thin-film electrode purchased from Adamant (at present, this material can be acquired from NeoCoat or Waterdiam), whereas the cathode was a carbon-polytetrafluoroethylene air-diffusion electrode purchased from E-TEK, mounted as described elsewhere [26] and fed with compressed air pumped at 1 L min^{-1} for continuous H_2O_2 generation from Reaction (2). The geometric area of each electrode was 3 cm^2 and the interelectrode gap was 1 cm. All experiments were carried out using 130 mL of solutions at pH 3.0 under vigorous stirring with a magnetic bar at 800 rpm to ensure homogenization and the transport of reactants towards/from the electrodes. In EF and PEF, 0.50 mM Fe^{2+}

was employed as catalyst because this content was found optimal for analogous treatments of aromatic azo dyes [16,29]. In PEF assays, the solution was irradiated with a Philips TL/6W/08 fluorescent black light blue tube (λ_{max} = 360 nm, photoionization energy of 5 W m^{-2}) placed 7 cm above the solution. Before the assays, cleaning of the BDD anode and activation of the air-diffusion electrode were achieved under polarization in 0.050 M Na_2SO_4 at 100 mA cm^{-2} for 180 min.

2.3. Apparatus and analytical procedures

The solution pH and the electrical conductance were measured with a Crison GLP 22 pH-meter and a Metrohm 644 conductometer, respectively. Trials were carried out at constant *j* provided by an EG&G PAR 273A potentiostat-galvanostat and the cell voltage was determined with a Demestres 601BR digital multimeter. Samples withdrawn from electrolyzed solutions were microfiltered with 0.45 μm PTFE filters purchased from Whatman prior to immediate analysis. The decolourization of Ponceau 4R solutions was monitored by measuring their absorbance decay at λ_{max} = 508 nm on a Shimadzu 1800 UV–vis spectrophotometer at 25 °C. The mineralization of solutions was assessed from their TOC abatement, determined on a Shimadzu TOC-VCNS analyser. Reproducible TOC values with an accuracy of ±1% were found by injecting 50 μL aliquots into the analyser.

The time course of the concentration of SO_4^{2-} and NO_3^- ions in trials in ultrapure water, as well as Cl^-, ClO_3^- and ClO_4^- ions in trials in real water, was assessed by ion chromatography (IC) as previously reported [43]. The decay of the dye concentration was followed by reversed-phase HPLC using a Waters 600 LC fitted with a Thermo Scientific Hypersil ODS 5 μm, 150 mm × 3 mm, column at room temperature and coupled with a Waters 996 photodiode array detector set at λ_{max} = 508 nm. A 80:20 (v/v) acetonitrile/water (2.4 mM butylamine) mixture at 0.2 mL min^{-1} was eluted as mobile phase. Generated carboxylic acids were detected by ion-exclusion HPLC as described elsewhere [40].

Electrolytic experiments were made in triplicate with a good reproducibility of all the data. Then, average results are given in all cases with standard deviations lower than 2%.

Well-defined peaks at characteristic retention times (t_r) were found in all cases: Cl^- (2.3 min), ClO_3^- (3.4 min), NO_3^- (3.8 min), SO_4^{2-} (5.2 min) and ClO_4^- (15.2 min) ions by IC, Ponceau 4R (4.3 min) by reversed-phase HPLC, and oxalic (6.9 min), tartronic (7.9 min), oxamic (9.4 min) and formic (13.7 min) acids by ion-exclusion HPLC.

Since only small traces of NH_4^+ ion, determined with a flow injection system [43], were found in all the experiments, the theoretical number of electrons (*n*) exchanged per each substrate molecule was taken as 102, assuming that Ponceau 4R is completely mineralized as follows:

$$C_{20}H_{11}N_2O_{10}S_3^{3-} + 48H_2O \rightarrow 20CO_2 + 2NO_3^- + 3SO_4^{2-} + 107H^+ + 102e^- \quad (8)$$

The mineralization current efficiency (MCE) values for each trial at current *I* (in A) and time *t* (in h) was then estimated as follows [37]:

$$MCE(\%) = \frac{(\Delta TOC)_{exp} n F V_s}{4.32 \times 10^7 m I t} \times 100 \quad (9)$$

where *F* is the Faraday constant (96,487 C mol^{-1}), V_s is the solution volume (in L), $\Delta(TOC)_{exp}$ is the experimental TOC abatement (in mg L^{-1}), 4.32×10^7 is a conversion factor to homogenize units (=3600 s h^{-1} × 12,000 mg carbon mol^{-1}) and *m* is the number of carbon atoms of Ponceau 4R.

To identify the aromatic by-products, various samples were withdrawn during the electrolyses and the organic components were extracted with CH_2Cl_2 (3 × 25 mL). In some cases, either derivatization with acetic anhydride or ethanol, or liofilization followed by overnight derivatization, were made prior to extraction. Each resulting organic solution was dried over anhydrous Na_2SO_4, filtered and concentrated up to 1 mL under reduced pressure to be analysed by gas chromatography-mass spectrometry (GC–MS) using an Agilent Technologies system composed of a 6890N chromatograph coupled to a 5975C spectrometer operating in EI mode at 70 eV. Nonpolar Agilent J&W DB-5ms and polar HP INNOWax columns (0.25 μm, 30 m × 0.25 mm) were employed. The temperature ramp was: 36 °C for 1 min, 5 °C min^{-1} up to 300 °C or 250 °C for the nonpolar and polar columns, respectively, and hold time of 10 min. The temperature of the inlet, source and transfer line was 250, 230 and 280 °C for the nonpolar column, and 250, 230 and 250 °C for the polar one. The mass spectra were identified by comparison with those of a NIST05 MS library.

3. Results and discussion

3.1. Electrochemical degradation of solutions of Ponceau 4R by PEF with a BDD anode

The treatment of organic pollutants by PEF is known to yield much better results than EF and EO–H_2O_2, which is mainly due to the synergistic action of UVA photons that induce photochemical Reactions (4) and (5). Therefore, acidic solutions of 254 mg L^{-1} (0.42 mM) of Ponceau 4R in ultrapure water with 0.05 M Na_2SO_4 as supporting electrolyte and 0.50 mM Fe^{2+} as catalyst were treated by PEF until reaching total decolourization using a BDD/air-diffusion cell. The initial solutions were bright red, as reported for other sulphonated monoazo dyes with two naphthalenes like Acid Red 14 and Acid Red 88 employed to impart red colour to food and textiles, respectively [41,44]. Fig. 1a shows the effect of applied *j* on the decay of normalized absorbance with electrolysis time. Solutions became colourless after 70, 60, 50 and 40 min at 33.3, 66.7, 100 and 150 mA cm^{-2}, respectively. Higher current values are then beneficial in such system in terms of time, since they promote both, the production of BDD(•OH) from Reaction (1) and H_2O_2 from Reaction (2) [37,41]. The quicker accumulation of the latter oxidant leads to a larger accumulation of •OH in the bulk at a given time from Reaction (3). Consequently, this radical species is the main responsible for the fast colour removal in Fenton systems, thanks to the minimization of mass transport limitations as compared to BDD(•OH) that can only act in the anode vicinity. Note that the enhancement obtained at 150 mA cm^{-2} was not very significant if compared to 100 mA cm^{-2}. This can be explained by the progressively lower current efficiency that results from: (i) the promoted cathodic and anodic destruction of H_2O_2 and (ii) the BDD(•OH) self-destruction to yield O_2 at excessively high current values. Quite frequently in literature, colour removal trends are directly associated to dye disappearance, but this is rarely verified because not enough attention is paid to reaction intermediates. Fig. 1b depicts the decay of normalized dye concentration with time during the same experiments. As found in Fig. 1a, a larger abatement was attained when *j* increased from 33.3 to 150 mA cm^{-2}, only requiring 40, 35, 30 and 25 min for total dye removal, respectively. This confirms the great oxidizing ability of PEF system, but it also reveals the formation of coloured by-products along the treatment because in all cases Ponceau 4R disappeared somewhat earlier than colour. Such compounds were poorly concentrated and/or exhibited small molar extinction coefficients. As shown in the inset panel of Fig. 1b, the concentration decays fitted very well to a pseudo-first-order kinetics with R^2 = 0.997 and increasing apparent rate constants

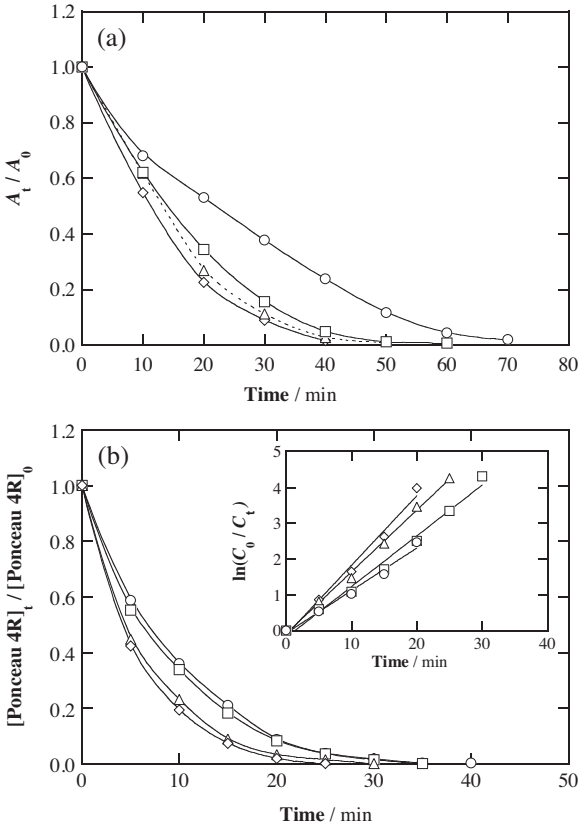

Fig. 1. Effect of applied current on the decay of the (a) normalized absorbance at 508 nm and (b) normalized dye concentration with electrolysis time for the degradation of 130 mL of a 254 mg L^{-1} (=0.42 mM) of Ponceau 4R solution in 0.050 M Na_2SO_4 at pH 3.0 and 25 °C by photoelectro-Fenton (PEF) process in the presence of 0.50 mM Fe^{2+} as catalyst. The cell contained a 3 cm^2 BDD anode and a 3 cm^2 air-diffusion cathode and the solution was irradiated with a 6 W UVA lamp of λ_{max} = 360 nm. Current density: (○) 33.3 mA cm^{-2}, (□) 66.7 mA cm^{-2}, (△) 100 mA cm^{-2} and (◊) 150 mA cm^{-2}.

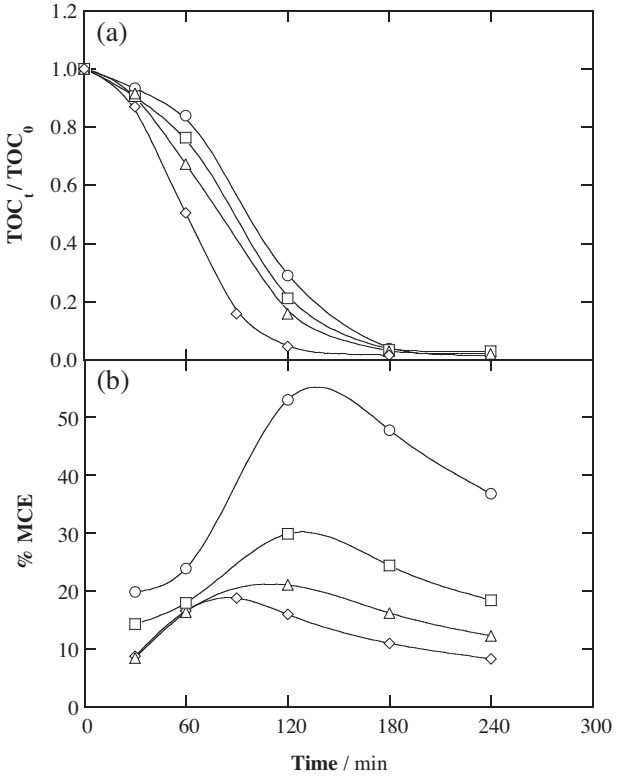

Fig. 2. Change of: (a) normalized TOC and (b) mineralization current efficiency with electrolysis time for the trials shown in Fig. 1.

(k_{app}, 10^{-2} min^{-1}) of 11.39 ± 1.74, 13.28 ± 1.26, 16.76 ± 0.96 and 18.60 ± 2.56 as *j* was raised from 33.3 to 150 mA cm^{-2} (mean values along with their computed 95% confidence intervals are provided). The good linearity can be accounted for by the accumulation of a constant concentration of hydroxyl radicals, both at the anode and in the bulk, at each applied *j*.

The time course of normalized TOC for the previous trials is presented in Fig. 2a. A sigmoid shape was observed in all cases, being the induction period more evident as *j* decreased. This is a symptom of the formation of refractory by-products since the very beginning of the electrolysis, which are slowly but progressively mineralized by BDD(•OH) and •OH. At high current, greater concentrations of both oxidizing radicals are produced, thus accelerating the TOC abatement. For example, TOC removals of 16%, 23%, 33% and 50% were obtained at 33.3, 66.7, 100 and 150 mA cm^{-2}, respectively, after 60 min of electrolysis. The degradation by PEF at 150 mA cm^{-2} was remarkably faster and, in fact, total mineralization was reached after only 180 min, whereas the electrolyses at 33.3–100 mA cm^{-2} had to be prolonged for 240 min to completely remove the organic matter (>99% TOC reduction). Worth mentioning, the tail of the sigmoid curves that is typical of mass transport limitation phenomena appeared at about TOC_t/TOC_0 = 0.20, which means that gradual cleavage of Ponceau 4R (and/or its aromatic by-products) easily yielded CO_2 according to mineralization Reaction (8), but an unavoidable accumulation of persistent free and iron-complexed by-products accounting for ca. 20% of TOC decelerated the degradation. Nonetheless, the use of UVA light allowed the slow destruction of such refractory compounds over time. The MCE values for the four experiments calculated from Eq. (9) are shown in Fig. 2b. As can be seen, after a poorly efficient early stage related to the aforementioned induction period, maximum MCE values of 55%, 29%, 21% and 18% were obtained after 90–120 min as current increased, whereupon the efficiency decayed due to the accumulation of by-products that were highly resistant to oxidation by BDD(•OH) and •OH and/or UVA photolysis. High current values are then preferred if time is the key parameter for applying the treatment, whereas such choice is detrimental in terms of energy consumption since parasitic reactions of BDD(•OH) and •OH are enhanced under such conditions, especially as the organic matter content diminishes [37–42].

Considering the usual variability of wastewater composition regarding the electrolyte content, it is interesting to investigate the effect of Na_2SO_4 concentration on PEF treatment. Fig. 3a shows the normalized absorbance decay over time at 33.3 mA cm^{-2} when using 0.010–0.30 M Na_2SO_4. As can be observed, total colour removal was always attained at 70 min. However, the extreme Na_2SO_4 concentration values yielded the quickest absorbance decays. It can then be deduced that 0.010 M Na_2SO_4 is sufficient so as to confer the threshold conductivity that allows an efficient production of BDD(•OH) and H_2O_2 at the anode and cathode, respectively. At that low SO_4^{2-} content, the parasitic anodic generation of the weaker oxidant $S_2O_8^{2-}$ is considerably minimized, therefore giving preponderance to the much more powerful BDD(•OH) [16]. Following this reasoning, a content as high as 0.30 M Na_2SO_4 could seem largely detrimental, since part of BDD(•OH) is expected to be wasted by the large formation of $S_2O_8^{2-}$ ion from the simultaneous SO_4^{2-} oxidation at the BDD anode [14]. Conversely, the presence of large amounts of SO_4^{2-} ions entails a considerable increase of the specific conductivity, which favours the transport of the negatively charged (sulphonated) Ponceau 4R molecules towards the anode surface, eventually accelerating their

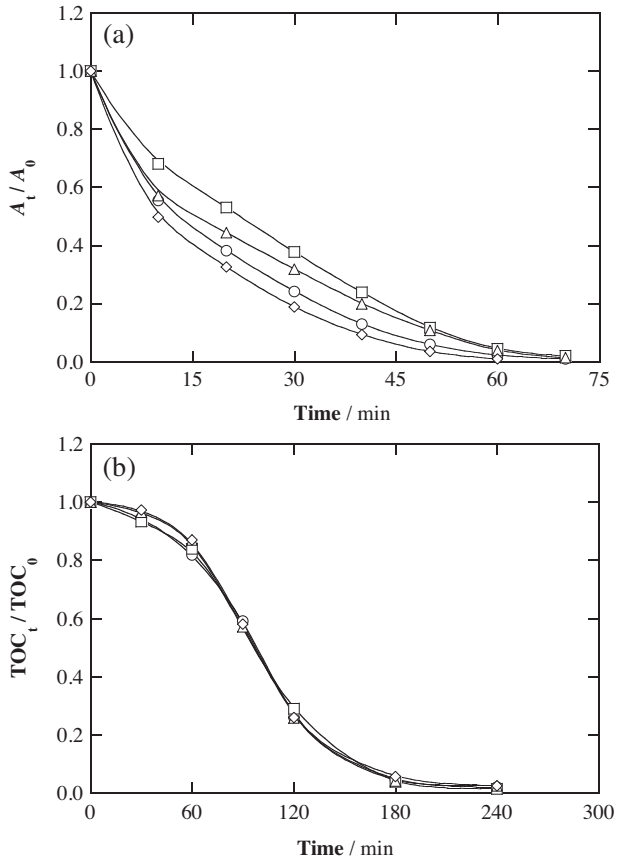

Fig. 3. Effect of supporting electrolyte concentration on the (a) normalized absorbance decay at 508 nm and (b) normalized TOC abatement vs electrolysis time for the degradation of 130 mL of 254 mg L^{-1} of Ponceau 4R solutions in: (○) 0.010 M, (□) 0.050 M, (△) 0.15 M and (◊) 0.30 M Na_2SO_4 with 0.50 mM Fe^{2+} at pH 3.0 and 25 °C by PEF with a BDD anode at 33.3 mA cm^{-2}.

oxidation. On the other hand, Fig. 3b reveals that the effect of the Na_2SO_4 concentration on TOC removal was negligible, leading to overlapped curves for 240 min. This can be justified by the conversion of Ponceau 4R into non-ionic, more refractory compounds, whose mineralization takes place pre-eminently in the solution bulk under the action of •OH from Fenton's Reaction (3) and/or photolysis by UVA photons from Reaction (5). Our results then point to consider that the BDD anode plays an important role during the initial decolourization steps, whereas Fenton's reaction and photolytic reactions ensure the progressive TOC abatement.

The effect of initial dye concentration on its decolourization and mineralization trends was examined for 127–1270 mg L^{-1} of Ponceau 4R (50–500 mg L^{-1} TOC) in 0.050 M Na_2SO_4 with 0.50 mM Fe^{2+} at 100 mA cm^{-2}. Fig. 4a depicts the complete decay of normalized absorbance with electrolysis time regardless of the dye content, which confirms the great oxidizing ability of PEF with BDD. Increasing times of 20, 50, 70 and 240 min were needed as the dye concentration rose from 127 to 1270 mg L^{-1}, which is simply due to the presence of larger amounts of coloured compounds that must react with a constant quantity of BDD(•OH) and •OH. Worth noting, the PEF treatment became more efficient as the organic matter content was raised. This behaviour arises from the greater probability for favourable events in the presence of more organic molecules, thus minimizing the parasitic reactions that involve BDD(•OH) and •OH. This can be more clearly seen in the trends of normalized TOC over time collected in Fig. 4b. Total abatement with >99% TOC reduction was attained in all cases, needing longer times of 135, 240, 360 and 480 min for 127, 254, 635 and 1270 mg L^{-1} of

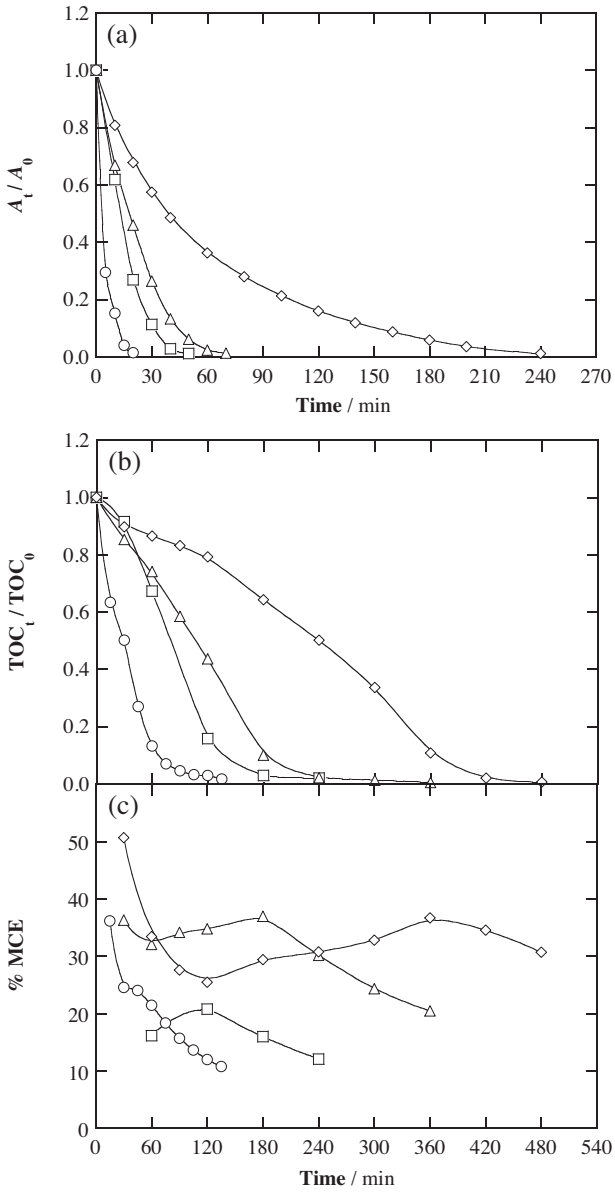

Fig. 4. Effect of dye concentration on the (a) normalized absorbance at 508 nm, (b) normalized TOC decay and (c) mineralization current efficiency with electrolysis time for the degradation of 130 mL of: (○) 127 mg L^{-1}, (□) 254 mg L^{-1}, (△) 635 mg L^{-1} and (◊) 1270 mg L^{-1} of Ponceau 4R solutions in 0.050 M Na_2SO_4 with 0.50 mM Fe^{2+} at pH 3.0 and 25 °C by PEF with a BDD anode at 100 mA cm^{-2}.

the dye, respectively. The MCE values for these trials depicted in Fig. 4c show an increase in the efficiency for more concentrated dye solutions, especially at long electrolysis time when the initial recalcitrant products were completely removed. Note that the TOC profile obtained for the greatest dye content exhibits an evident shoulder (see Fig. 4b), which is indicative of the progressively larger difficulties to remove the organic matter. This resulted in a minimum MCE value at 120 min, although it further reached the highest efficiencies, which were close to 35% at times > 240 min (see Fig. 4c). Several phenomena can be responsible for the deceleration of degradation in Fenton systems at excessively high organic matter contents, including iron complexation upon generation of many aliphatic by-products, polymerization and partial blockage of the electrode surfaces that causes passivation [29].

3.2. Reaction by-products and proposed routes

As observed in Figs. 2 a, 3 b and 4 b, the final stages of the PEF treatment were characterized by a lower mineralization rate. This kind of behaviour has been usually associated to the formation of polymers as well as short-chain carboxylic acids, whose absolute rate constants for their reaction with hydroxyl radicals tends to be much smaller than those exhibited by aromatic compounds [16,29]. In the present study, HPLC analyses of samples withdrawn from PEF experiments at 100 mA cm^{-2} revealed the formation of up to 0.02 and 0.28 mM of tartronic and formic acids, respectively, although they were easily mineralized under the action of BDD(•OH) and •OH regardless of the formation of iron complexes [29]. A more particular situation was found for oxalic and oxamic acids, whose concentration profiles with time are shown in Fig. 5a and b, respectively. Oxalic acid was accumulated up to a maximum content of 0.45 mM at 60 min, whereupon it gradually decayed up to its total disappearance at 180 min. A much smaller amount of oxamic acid was formed, only reaching up to 0.014 mM at 90 min with total degradation at 210 min. These two findings agree with the mentioned high oxidizing ability of the PEF process with a BDD anode (see the corresponding TOC evolution in Fig. 2a), which can then be justified by the effective degradation of both acids and the Fe(II)-carboxylate complexes under the action of BDD(•OH) and •OH, along with the efficient photodegradation of Fe(III)-oxalate and Fe(III)-oxamate complexes by UVA photons [29]. Clearly different profiles were obtained upon comparative treatment of analogous Ponceau 4R solutions by EF and EO–H_2O_2 with a BDD anode, which allowed the complete mineralization at 480 min but only 80% and 65% TOC removal at 240 min, respectively (not shown). In the former method, the maximum concentrations of oxalic and oxamic acids were found at 90–120 min (0.88 and 0.012 mM, respectively, see Fig. 5). Due to the large persistence of oxalic/oxalates, its total abatement was only ensured after 480 min of EF, whereas oxamic acid disappeared at 270 min. This confirms the crucial role of UVA radiation, which was responsible for the lower accumulation and faster removal in PEF. As reported elsewhere, Fe(III)-oxalate complexes are quite refractory to •OH formed in the bulk and thus, in EF, only BDD(•OH) is able to slowly oxidize them. On the other hand, very small amounts of oxalic (≤0.05 mM) and oxamic (≤0.005 mM) were detected in EO–H_2O_2, which can be explained by the absence of iron complexes, therefore favouring the quick oxidation of all by-products by BDD(•OH). In conclusion, the extraordinary ability of PEF with BDD to quickly degrade both, the parent pollutant and its coloured and colourless reaction by-products, allows explaining the superior performance of this process as compared to the other EAOPs. Note that GC–MS analyses of treated solutions allowed the identification of other aliphatic acids like maleic, fumaric, tartaric and propanoic acids, which were not detected by ion-exclusion HPLC due to their quick removal and very small accumulation.

Inorganic ions formed during the electrolyses were determined by IC. The N atoms forming the —N=N— bond were preferentially detected as NO_3^- ion (50% of initial N) and, to a smaller extent, as NH_4^+ ion (25%), as stated in Reaction (8). A significant proportion of the initial N was then lost as volatile nitrogenated products, like N_2 and N_xO_y, as reported for similar treatments of other azo dyes [41,42,44]. Regarding the sulfur content, the initial S atoms were mainly released as SO_4^{2-} ion. Fig. 6 depicts its time course during the degradation of 254 mg L^{-1} Ponceau 4R (0.42 mM) solutions in 0.05 M $LiClO_4$. As can be seen in Fig. 6a, in PEF, almost 1 mM SO_4^{2-} was accumulated after 50 min (80% of initial S). At that time, no coloured sulphonated by-products were present in the solutions (see Fig. 1a), which means that S was contained in either sulphonated aliphatic compounds or colourless aromatics. All of them were quickly oxidized and/or photolyzed and, at the end of the treatment, ca. 100% of S (1.25 mM) was found as SO_4^{2-}. The

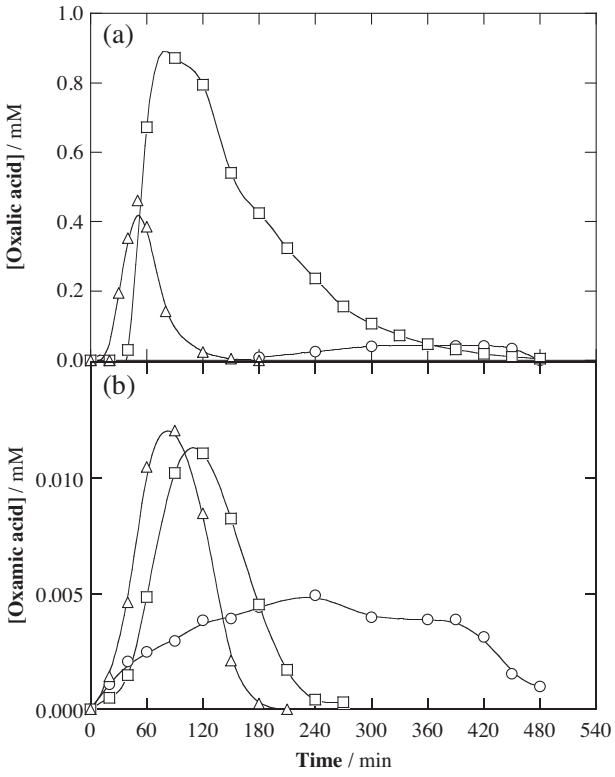

Fig. 5. Evolution of the concentration of (a) oxalic and (b) oxamic acids detected during the degradation of 130 mL of 254 mg L^{-1} of Ponceau 4R solutions in 0.050 M Na_2SO_4 at pH 3.0, 25 °C and 100 mA cm^{-2}. Methods with a BDD anode: (○) EO-H_2O_2, (□) EF with 0.50 mM Fe^{2+} and (△) PEF with 0.50 mM Fe^{2+}.

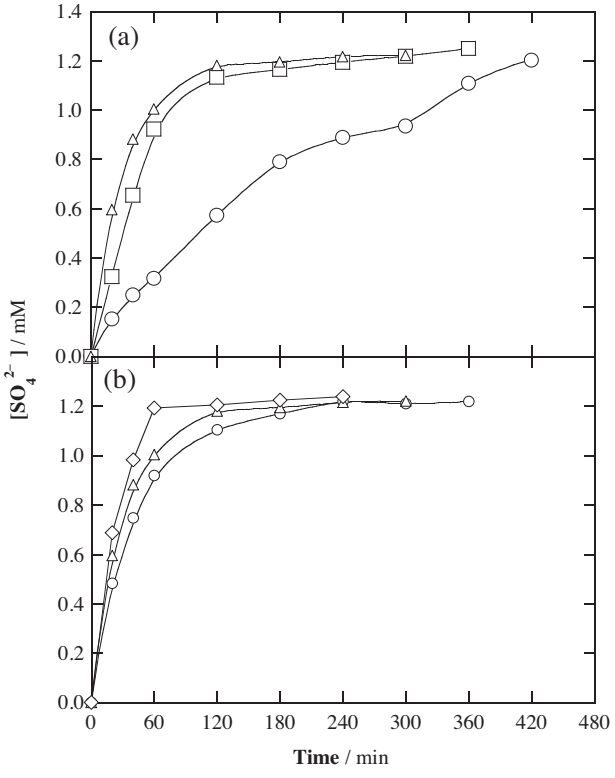

Fig. 6. Time course of the concentration of SO_4^{2-} ions released during the degradation of 130 mL of 254 mg L^{-1} of Ponceau 4R solutions in 0.050 M $LiClO_4$ at pH 3.0 and 25 °C with a BDD anode. In (a), (○) EO-H_2O_2, (□) EF with 0.50 mM Fe^{2+} and (△) PEF with 0.50 mM Fe^{2+} at 100 mA cm^{-2}. In (b), PEF with 0.50 mM Fe^{2+} at: (○) 33.3 mA cm^{-2}, (△) 100 mA cm^{-2} and (◊) 150 mA cm^{-2}.

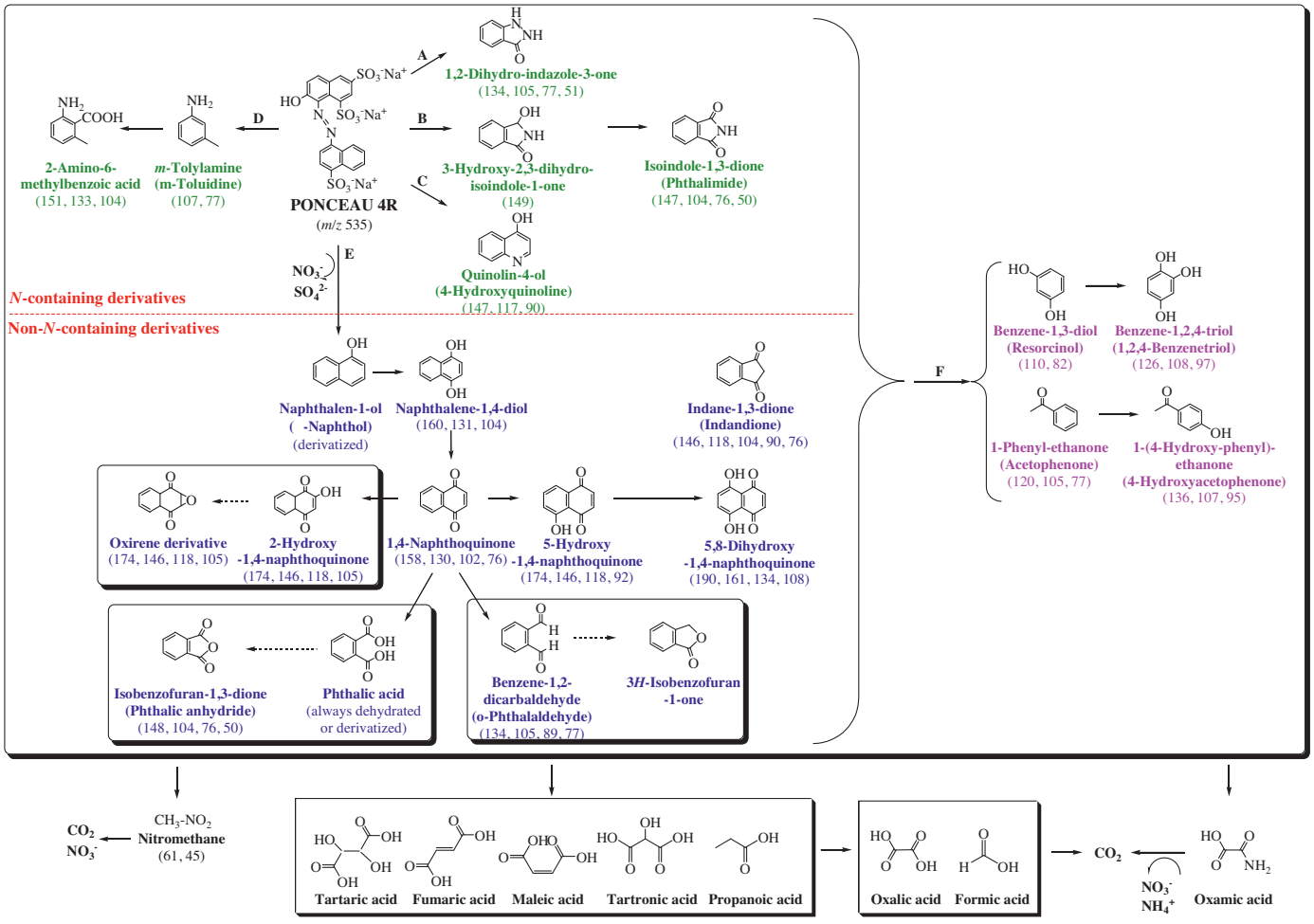

Fig. 7. Routes for the electrolytic degradation of Ponceau 4R in acidic aqueous medium by EAOPs with BDD anode. The primary oxidation by-products, as well as some of the final aliphatic intermediates, were identified by GC–MS.

trend of this ion was analogous in EF, which means that UVA light mainly affects the non-sulphonated carboxylic acids, as discussed above. A much slower accumulation was obtained in EO–H_2O_2, only attaining the expected SO_4^{2-} concentration after prolonged electrolysis. This confirms the great contribution of •OH to mineralization, since its absence in the latter method yields lower degradation rates. On the other hand, an increase in j from 33.3 to 150 mA cm^{-2} in PEF led to a faster accumulation of SO_4^{2-} ions, as expected from the quicker generation of BDD(•OH) and •OH but, in all cases, this ion accounted for the release of ca. 100% of S at the end of all the treatments.

Apart from revealing the formation of some additional aliphatic carboxylic acids, as mentioned before, GC–MS analyses of treated solutions with polar and nonpolar columns allowed the identification of nitromethane as well as various aromatic by-products. Their structures, chemical names and characteristic m/z values have been gathered in Fig. 7, which constitutes a proposal of different degradation routes for the electrolytic degradation of Ponceau 4R in acidic aqueous medium by EO–H_2O_2, EF and PEF with a BDD anode. The final aliphatic intermediates formed upon successive cleavage are also included.

Ponceau 4R appears with m/z 535, which corresponds to its anionic form without the sodium counterions. Its degradation may proceed through the formation of up to six *N*-containing derivatives (highlighted in green) following four different routes (A–D). A–C inform about the appearance of four *N*-based heterocycles, which can be plausibly produced upon primary radical formation from electron transfer at the cathode (so-called electrochemically-induced radical cyclization [45]). Path A involves intramolecular cyclization, path B arises from intermolecular cyclization as suggested by the presence of an additional carbon to close the *N*-cycle and path C comes from intra or intermolecular cyclization because some of the carbon atoms of benzene might allow closing the *N*-cycle. Among all the heterocycles, phthalimide was the most ubiquitous one. Conversely, route D leads to two aromatic amines, which were typically formed when a stainless steel cathode was used instead of the air-diffusion electrode, thus confirming the purely oxidative degradation underwent by the azo dye in systems with BDD/air-diffusion cells.

Alternatively, Ponceau 4R can follow route E to yield up to twelve non-*N*-containing derivatives (highlighted in blue) with one or two cycles, starting with its conversion to α-naphthol. As observed, this compound is the source of most of these by-products, except indandione, via 1,4-naphthoquinone. Discontinuous arrows account for transformations that can take place or rather be GC–MS artifacts, being impossible to elucidate the exact by-product in each case. Ponceau 4R, as well as its eighteen aromatic by-products, can be further transformed into non-*N*-containing derivatives with one cycle, such as resorcinol, acetophenone and their hydroxylated by-products following route F (highlighted in pink). Worth mentioning, a condensation reaction involving acetophenone could potentially yield indandione, as occurs in well-known aldol condensation. The cleavage of any of the 22 aromatic structures caused the formation of aliphatic compounds, which

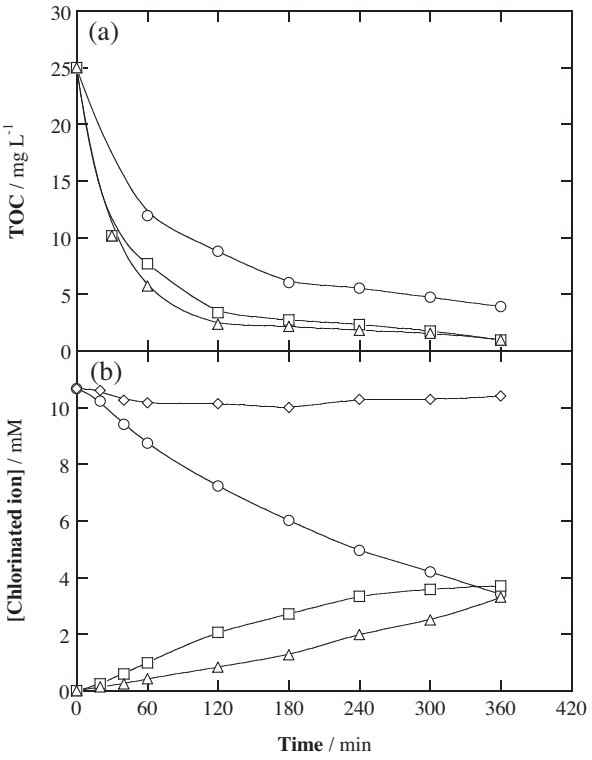

Fig. 8. Performance of the EAOPs with a BDD anode during the treatment of 130 mL of a real water sample at pH 3.0, 25 °C and 33.3 mA cm^{-2}. (a) TOC removal by (○) EO-H_2O_2, (□) EF with 0.50 mM Fe^{2+} and (△) PEF with 0.50 mM Fe^{2+}. (b) Time course of the concentration of chlorinated ions accumulated in PEF process. (○) Cl^-, (□) ClO_3^-, (△) ClO_4^- and (◊) sum of chlorinated ions.

were finally mineralized to CO_2 under optimized electrolysis conditions.

Some of the intermediates proposed in this work are consistent with those obtained during the degradation of other azo dyes. For example, the treatment of Acid Orange 7, which includes a phenylazonaphthol group, by TiO_2 photocatalysis yielded naphthol, naphthalene-1,4-diol, 1,4-naphtoquinone, hydroxynaphthoquinone, phthalic anhydride, 3*H*-isobenzofuran-1-one (phthalide) and phthalimide [46].

3.3. Treatments with a BDD anode in a real water matrix

The great performance of EAOPs with a BDD anode, particularly PEF, regarding the decontamination of acidic Ponceau 4R solutions has been demonstrated for pure water matrices. However, real dye wastewater is not so ideal because it usually contains natural organic matter and various inorganic anions, which may hamper the application of those technologies. Therefore, some experiments were carried out using a real water matrix (see Section 2.1). First, the raw real water samples (TOC = 25 mg L^{-1}) were treated at 25 °C and 33.3 mA cm^{-2} in the absence of the dye by EO–H_2O_2, EF and PEF. Prior to the electrolyses, the initially alkaline pH was adjusted to 3.0, and 0.50 mM Fe^{2+} was added to the solutions for the two latter treatments. The time course of natural TOC with time is shown in Fig. 8a. EO–H_2O_2 allowed a significant TOC abatement thanks to the action of BDD(•OH) on organic matter, eventually reaching 86% mineralization at 360 min. TOC removal was accelerated in EF from the beginning of the treatment, with >95% mineralization at 360 min. This suggests that the catalytic amount of Fe^{2+} favours the formation of •OH during all the electrolysis, notwithstanding the plausible partial complexation of iron ions by chelating species contained in the water sample. The rate and degree of mineralization was very similar in the case of PEF process, which means that photosensitive Fe(III) complexes such as Fe(III)-oxalate species were not formed to a large extent along the treatment.

Since the water sample contained about 2.0 mM SO_4^{2-} and 10.3 mM Cl^-, some oxychlorine anions were formed under the oxidative action of BDD, BDD(•OH) and •OH [30–32]. As an example, the evolution of chlorinated ions in PEF process is illustrated in Fig. 8b. The Cl^- concentration gradually decreased to 3.4 mM at 360 min, owing to its transformation into ClO_3^- (3.6 mM) and ClO_4^- (3.3 mM) ions. As can be observed, such conversion was quite quantitative because the sum of the three anions accounted for almost 100% of the initial Cl content. This suggests a very small accumulation of active chlorine from Reactions (6) and (7) and therefore, the mineralization of organic matter in Fig. 8a can be essentially explained by the participation of hydroxyl radicals. Furthermore, the accumulation of Cl in the form of chlorinated anions ensures that the generation of toxic chlorinated organic by-products during the treatment can be neglected.

The performance of the three EAOPs during the degradation of 254 mg L^{-1} of Ponceau 4R in the same real water matrix of Fig. 8, at pH 3.0 and 33.3 mA cm^{-2}, was further assessed. Fig. 9a presents the decay of the normalized absorbance achieved by EO–H_2O_2, EF and PEF in the absence or presence of added electrolyte. When treating the dye in the raw water, total colour removal was attained after 180, 100 and ca. 70 min, respectively, in agreement with the higher oxidizing ability in the sequence EO–H_2O_2 < EF < PEF. Note that the time needed in PEF is similar to that found in Fig. 1a for the treatment under analogous conditions but using ultrapure water, which means that the water matrix does not impede the fast decolourization of the dye solutions. Actually, the real matrix was even beneficial, since 50% colour removal was reached after 10–15 min of PEF instead of 25 min required in ultrapure water (see Fig. 1a). This suggests the contribution of active chlorine to the oxidation of coloured compounds, despite the very small accumulation of such oxidant (see Fig. 8b). The participation of active chlorine was more evident when the PEF treatment was performed in the presence of 0.010 M NaCl, which allowed a quicker decolourization with total disappearance of coloured compounds at 60 min. In contrast, the addition of 0.010 M Na_2SO_4 did not enhance the process, but it was slightly detrimental by the formation of competitive $S_2O_8^{2-}$ ion.

The decay of the normalized dye concentration for the experiments of Fig. 9a without added electrolyte is shown in Fig. 9b, along with the corresponding kinetic analysis assuming a pseudo-first-order reaction. Ponceau 4R disappeared after 140 min in EO–H_2O_2, only requiring about 40 min in EF and PEF, thus confirming the superiority of Fenton processes due to the much faster reaction of the azo dye with •OH formed from Fenton's reaction (3). The mean values of k_{app} (10^{-2} min^{-1}) with their 95% confidence intervals were 2.72 ± 0.41, 12.31 ± 0.53 and 13.35 ± 0.66 for EO–H_2O_2, EF and PEF, respectively. As also observed in Fig. 1, the time needed for removing the dye was lower than that for colour removal. Note that Ponceau 4R disappeared at the same time in both, ultrapure (see Fig. 1b) and real water matrices (see Fig. 9b), indicating a small participation of active chlorine.

Finally, Fig. 9c shows the TOC removal during all the trials of Fig. 9a. At 360 min, 57%, 74% and ~100% mineralization was attained by EO–H_2O_2, EF and PEF, respectively. This result, along with the fast colour and Ponceau 4R removals, verifies the viability of PEF process for the treatment of real wastewater. Comparison with the TOC abatement in ultrapure water (see Fig. 2a), where total mineralization was reached after 240 min, allowed concluding that the degradation proceeded somewhat more slowly, with 93% TOC decay at that time. This can be explained by: (i) the presence of a larger amount of organic matter due to the natural constituents, (ii) the partial consumption of BDD(•OH) by Cl^- to form less oxidizing species [30–33], (iii) the partial destruction of H_2O_2 by HClO

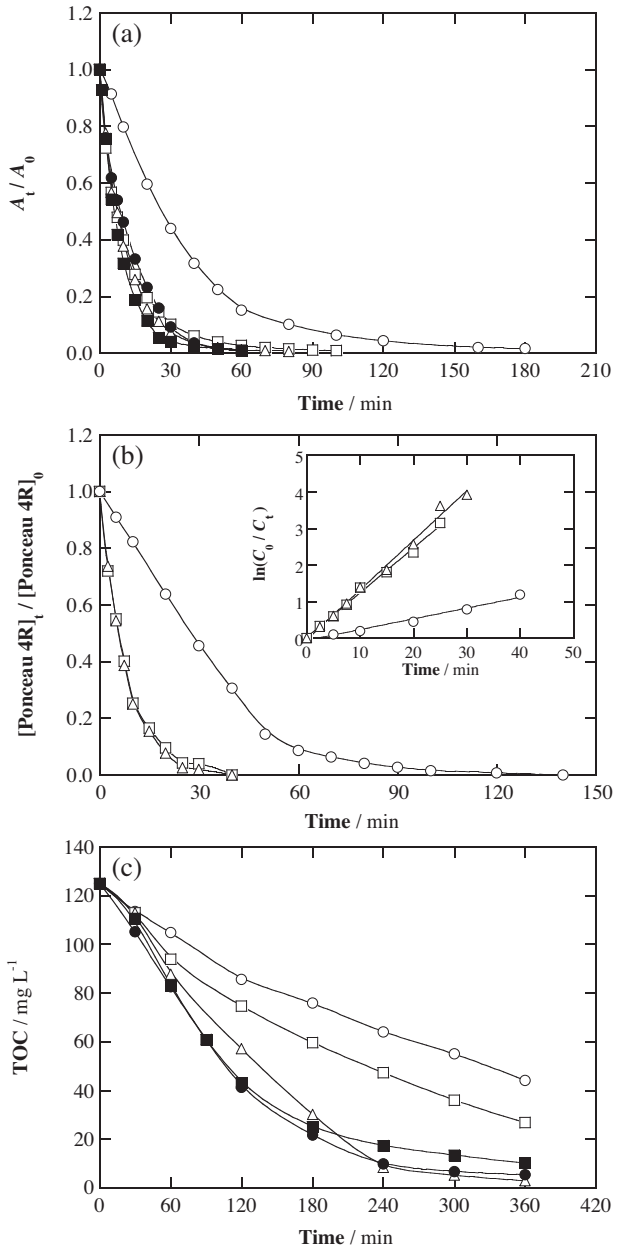

Fig. 9. Performance of the EAOPs with a BDD anode during the degradation of 130 mL of 254 mg L^{-1} of Ponceau 4R in the same real water matrix of Fig. 8, at pH 3.0, 25 °C and 33.3 mA cm^{-2}. (a) Decay of the normalized absorbance at 508 nm without added electrolyte by (○) EO–H_2O_2, (□) EF with 0.50 mM Fe^{2+} and (△) PEF with 0.50 mM Fe^{2+}, and with addition of (●) 0.010 M Na_2SO_4 or (■) 0.010 M NaCl in PEF. (b) Decay of the normalized dye concentration in the experiments without added electrolyte. (c) TOC removal during the trials shown in plot (a).

formed via Reactions (6) and (7) [32] and (iv) the formation of chloro-complexes that reduce the amount of free iron ions [47]. While the presence of Cl^- resulted positive for colour removal (see Fig. 9a), it became detrimental regarding the TOC abatement. This was confirmed when treating the dye in the presence of 0.010 M NaCl, since only 82% and 92% mineralization could be attained after 240 and 360 min of PEF, respectively. In contrast, the effect of added Na_2SO_4 was insignificant, as discussed above.

4. Conclusions

Iron-catalyzed PEF treatment using a BDD/air-diffusion cell has been proven a promising technology for the degradation of food azo-colours like Ponceau 4R contained in real water matrices thanks to the synergistic action of BDD(•OH), •OH and UVA photons. No significant detrimental effects of the real matrix were observed, since the time required for the complete dye and colour removals was comparable to that needed in ultrapure water, whereas only a slight deceleration of TOC decay was revealed as a result of parasitic reactions induced by the presence of Cl^-. Up to 22 aromatic by-products, 8 carboxylic acids and nitromethane were identified upon treatment of Ponceau 4R by EAOPs with BDD. The total mineralization of all these by-products to yield CO_2, NO_3^-, NH_4^+ and SO_4^{2-} proceeded via various simultaneous reaction routes.

Acknowledgments

The authors thank MINECO (Ministerio de Economía y Competividad, Spain) for financial support under project CTQ2013-48897-C2-1-R, co-financed with FEDER funds. The Ph.D. grant awarded to A. Thiam from MAEC-AECID (Spain) is also acknowledged.

References

[1] IFIC and FDA, Food ingredients and colors, pp. 1–7 (http://www.fda.gov/downloads/Food/IngredientsPackagingLabeling/ucm094249.pdf; November 2004, revised April 2010).
[2] I.K. Konstantinou, T.A. Albanis, Appl. Catal. B Environ. 49 (2004) 1–14.
[3] E. Brillas, C.A. Martínez-Huitle, Appl. Catal. B Environ. 166–167 (2015) 603–643.
[4] D. McCann, A. Barrett, C. Cooper, D. Crumpler, L. Dalen, K. Grimshaw, E. Kitchin, K. Lok, L. Porteous, E. Prince, E. Sonuga-Barke, J. O'Warner, J. Stevenson, Lancet 370 (2007) 1560–1567.
[5] EFSA, EFSA J. 7 (2009) 1328–1366.
[6] L.E. Arnold, N. Lofthouse, E. Hurt, Neurotherapeutics 9 (2012) 599–609.
[7] http://www.fda.gov/ForIndustry/ColorAdditives/ColorAdditiveInventories/ucm115641.htm
[8] M.M. Ghoneim, H.S. El-Desoky, N.M. Zidan, Desalination 274 (2011) 22–30.
[9] K. Tanaka, K. Padermpole, T. Hisanaga, Water Res. 34 (2000) 327–333.
[10] N. Sobana, M. Swaminathan, Sep. Purif. Technol. 56 (2007) 101–107.
[11] J. Basiri Parsa, M. Golmirzaei, M. Abbasi, J. Ind. Eng. Chem. 20 (2014) 689–694.
[12] K. Barbusiński, J. Majewski, Pol. J. Environ. Stud. 12 (2003) 151–155.
[13] C. Benincá, P. Peralta-Zamora, R.C. Camargo, C.R.G. Tavares, E.F. Zanoelo, L. Igarashi-Mafra, Reac. Kinet. Mech. Cat. 105 (2012) 293–306.
[14] M. Panizza, G. Cerisola, Chem. Rev. 109 (2009) 6541–6569.
[15] B.P. Chaplin, Environ. Sci. Process. Impacts 16 (2014) 1182–1203.
[16] I. Sirés, E. Brillas, M.A. Oturan, M.A. Rodrigo, M. Panizza, Environ. Sci. Pollut. Res. 21 (2014) 8336–8367.
[17] L. Ciríaco, C. Anjo, J. Correia, M.J. Pacheco, A. Lopes, Electrochim. Acta 54 (2009) 1464–1472.
[18] M.A. Rodrigo, P. Cañizares, A. Sánchez-Carretero, C. Sáez, Catal. Today 151 (2010) 173–177.
[19] A. El-Ghenymy, F. Centellas, J.A. Garrido, R.M. Rodríguez, I. Sirés, P.L. Cabot, E. Brillas, Electrochim. Acta 130 (2014) 568–576.
[20] M. Panizza, Environ. Sci. Pollut. Res. 21 (2014) 8451–8456.
[21] O. Scialdone, E. Corrado, A. Galia, I. Sirés, Electrochim. Acta 132 (2014) 15–24.
[22] M.J.M.D. Vidales, S. Barba, C. Sáez, P. Cañizares, M.A. Rodrigo, Electrochim. Acta 140 (2014) 20–26.
[23] D.M.D. Araújo, C. Sáez, C.A. Martínez-Huitle, P. Cañizares, M.A. Rodrigo, Appl. Catal. B Environ. 166–167 (2015) 454–459.
[24] A. Özcan, Y. Sahin, A.S. Koparal, M.A. Oturan, J. Electroanal. Chem. 616 (2008) 71–78.
[25] E. Rosales, M. Pazos, M.A. Longo, M.A. Sanromán, Chem. Eng. J. 155 (2009) 62–67.
[26] E. Guinea, J.A. Garrido, R.M. Rodríguez, P.L. Cabot, C. Arias, F. Centellas, E. Brillas, Electrochim. Acta 55 (2010) 2101–2115.
[27] M. Panizza, M.A. Oturan, Electrochim. Acta 56 (2011) 7084–7087.
[28] A. Dirany, I. Sirés, N. Oturan, A. Özcan, M.A. Oturan, Environ. Sci. Technol. 46 (2012) 4074–4082.
[29] E. Brillas, I. Sirés, M.A. Oturan, Chem. Rev. 109 (2009) 6570–6631.
[30] M.E. Bergmann, J. Rollin, Catal. Today 124 (2007) 198–203.
[31] A.M. Polcaro, A. Vacca, M. Mascia, S. Palmas, J. Rodriguez Ruiz, J. Appl. Electrochem. 39 (2009) 2083–2092.
[32] S. Randazzo, O. Scialdone, E. Brillas, I. Sirés, J. Hazard. Mater. 192 (2011) 1555–1564.
[33] F. Bonfatti, S. Ferro, F. Lavezzo, M. Malacarne, G. Lodi, A. De Battisti, J. Electrochem. Soc. 147 (2000) 592–596.
[34] M. Deborde, U. von Gunten, Water Res. 42 (2008) 13–51.
[35] S.D. Richardson, Global NEST J. 7 (2005) 43–60.
[36] M. Panizza, G. Cerisola, Ind. Eng. Chem. Res. 47 (2008) 6816–6820.

[37] E.J. Ruiz, C. Arias, E. Brillas, A. Hernández-Ramírez, J.M. Peralta-Hernández, Chemosphere 82 (2011) 495–501.
[38] L.C. Almeida, S. Garcia-Segura, C. Arias, N. Bocchi, E. Brillas, Chemosphere 89 (2012) 751–758.
[39] R. Salazar, E. Brillas, I. Sirés, Appl. Catal. B Environ. 115–116 (2012) 107–116.
[40] F.C. Moreira, S. Garcia-Segura, V.J.P. Vilar, R.A.R. Boaventura, E. Brillas, Appl. Catal. B Environ. 142–143 (2013) 877–890.
[41] A. Thiam, I. Sirés, J.A. Garrido, R.M. Rodríguez, E. Brillas, Sep. Purif. Technol. 140 (2015) 43–52.
[42] A. Thiam, I. Sirés, J.A. Garrido, R.M. Rodríguez, E. Brillas, J. Hazard. Mater. 290 (2015) 34–42.
[43] A.R.F. Pipi, A.R. De Andrade, E. Brillas, I. Sirés, Sep. Purif. Technol. 132 (2014) 674–683.
[44] E.J. Ruiz, A. Hernández-Ramírez, J.M. Peralta-Hernández, C. Arias, E. Brillas, Chem. Eng. J. 171 (2011) 385–392.
[45] S. Donnelly, J. Grimshaw, J. Trocha-Grimshaw, Electrochim. Acta 41 (1996) 489–492.
[46] M. Stylidi, D.I. Kondarides, X.E. Verykios, Appl. Catal. B Environ. 40 (2003) 271–286.
[47] J. De Laat, G.T. Le, B. Legube, Chemosphere 55 (2004) 715–723.